NMR study of photo-crosslinked solid polymer electrolytes: The influence of monofunctional oligoethers

NMR study of photo-crosslinked solid polymer electrolytes: The influence of monofunctional oligoethers

Annalisa Chiappone[1]*[a], Sebastian Jeremias[1] [b], Roberta Bongiovanni [a], Monika Schönhoff [b]

Received (in XXX, XXX) Xth XXXXXXXXX 20XX, Accepted Xth XXXXXXXXX 20XX
DOI: 10.1039/b000000x

Solid polymer electrolytes for Lithium batteries applications are commonly prepared by dissolving a lithium salt in poly(ethylene oxide) (PEO) based materials. Their performance is strongly related to the structure of the polymer network. In this paper we investigate new salt-in-polymer electrolytes prepared by the fast and easy radical photopolymerisation of PEO acrylate oligomers. Here, a difunctional monomer used as the polymer backbone is co-polymerised with monofunctional monomers of different length and concentration. Thus, the crosslinking density and conductivity are changed. These systems are investigated by a detailed NMR study yielding local dynamics and mass transport by temperature dependent spin-lattice relaxation time and PFG-NMR diffusion measurements for different nuclei (^{7}Li and ^{19}F). The results indicate that a sufficiently long monofunctional oligoether improves the properties, since it provides a lower crosslinking density as well as more coordinating oxygens for the Li ions.

[1] Both authors contributed equally.

Introduction

The constantly increasing energy demand is creating the necessity to look for new, more efficient, safe and low cost alternatives to fossil fuel resources like renewable energy and suitable rechargeable energy storage devices in order to deliver problem-free solutions.

Li-based battery systems, traditionally limited to the field of portable electronic devices, have undergone in recent years a rapid and substantial improvement.[1-4] High production volumes, low cost, ecological friendliness and high safety standards, in addition to high specific performance, are key factors in the choice of the device. The progress in the field of Li batteries is based on the development and on the continuous research of new materials for the cathode and the anode and for the electrolyte. The latter component has undergone in the last years a complete transformation from all-liquid to all-solid and it has still good perspectives of improvement. Polymer electrolytes represent the ultimate in terms of desirable properties of Li-based batteries because they can offer an all-solid-state construction, a wide variety of shapes and sizes, light-weight, low cost of fabrication and a higher energy density. No corrosive or explosive liquids can leak out and internal short-circuits are less likely, hence greater safety is guaranteed. All these attractive features make lithium polymer batteries the power sources of choice for the next generation of lightweight consumer devices.[5, 6] Solid polymer electrolytes for Lithium batteries are usually prepared by dissolving a lithium salt in poly(ethylene oxide) (PEO) based materials: this process requires long time. An interesting alternative is to dissolve the salt in liquid monomers and then polymerise them in situ. A fast and reliable method is the photoinduced polymerisation, usually employing UV light. If the reactive monomers are multifunctional, crosslinking takes place. The principle of UV curing is based on initiating a chemical polymerisation inside a liquid poly-functional monomer containing a proper photo-initiator using direct UV irradiation to create a highly cross-linked, dry, solid film. A typical formulation may consist of more than one monomer and oligomer, but typically is solvent free. The irradiation time ranges from few seconds to few minutes and light is the only energy source for building up the polymeric thermo-set matrix. Therefore, the process is well known for being fast, economic and environmentally friendly, as the energy consumption is low and there is no emission of volatile organic compounds.[7] Thermo-set membranes prepared by photo polymerization (UV curing) have proved to represent an interesting alternative to the present processing methods. First results were published by Song and co-workers[8] who prepared chemically and physically cross-linked polyethylenglycoldiacrylate-PVDF blend gel-electrolytes of high ionic conductivity. In line with this tendency, in the recent years a series of polymer electrolyte membranes [9, 10, 11] were also made from different difunctional acrylic / methacrylic formulations with mono-functional methacrylates and also some surface modifications by siloxane diacrylates were investigated[12], all providing good results in terms of electrochemical performance. To further improve this kind of polymer-gel electrolytes, the membrane formulation can be optimized and/or new acrylic networks can be synthesized.

For a purposeful choice of the architectures to be built it is necessary to understand in depth the factors affecting the performance of the membranes, i.e. the parameters influencing the ion mobility and the transport processes in such systems. Ion dynamics can be studied by multinuclear dynamic NMR experiments.[13-16] In particular, spin-lattice relaxation and diffusion studies are well established in salt-in-polymer electrolytes.[17-26] The relaxation of nuclear spins depends on the spectral density function, which describes dynamic fluctuations of the local environment of a nucleus. By determining spin-lattice relaxation rates R_1 and applying appropriate motional models, the local dynamics of a nucleus is characterized by its motional correlation time. While for protons in organic material a complex superposition of dipolar interaction allows only a qualitative characterisation, in the case of quadrupolar nuclei with a defined local interaction, relaxation rates R_1 yield quantitative values of local motional correlation times.[27]

In addition to this, Pulsed Field Gradient-NMR (PFG- NMR) can be applied to determine mean square displacements and thus the diffusion coefficients of the nuclei under observation. Since the observation time is typically in the range of 10 ms to 500 ms, the root mean square displacement is on the order of µm; therefore the diffusion coefficients can monitor the molecular transport over long range dimensions and give valuable information on local mobility.[28, 29]

In this work we present spin relaxation and PFG-NMR studies on new photo-cured acrylic membranes, the results obtained from the NMR studies can be linked to the polymer architecture. In particular, we varied the concentration and length of an added monofunctional unit and we could modulate the crosslinking density of the system in this way. We show that the expected variation in turn influences local ion mobility and ion transport in different ways.

Experimental part

Materials.

The reactive oligomer for the preparation of the solid polymer electrolyte membranes was based on poly(ethylene glycol)diacrylate (13 EO) PEGDA, (see Figure 1), an acrylic based di-functional oligomer having an average molecular weight of 700, obtained from Aldrich. As a comonomer a poly(ethylene glycol) phenyl ether acrylate (see Figure 1) with different molecular weights i.e. $PEEA^{236}$, $PEEA^{324}$ having average M_n of 236 (2 EO units) and 324 (4 EO units), respectively, were used (Aldrich). Bis(trifluoromethane)sulfonimide lithium salt (LiTFSI, $CF_3SO_2NLi\text{-}SO_2CF_3$), battery grade (Ferro Corp. (USA), was used as the source of Li^+ ions. The free radical photo-initiator was 2-hydroxy-2-methyl-1-phenyl-1-propanone (Darocur 1173/ D1173), provided by Ciba Specialty Chemicals.

Before their use, all chemicals were kept open in the inert atmosphere of an Ar-filled dry glove box for several days and were also treated with molecular sieves (Molecular sieves, beads 4 Å, 8–12 mesh, Aldrich) to ensure the complete removal of traces of water/moisture.

Sample preparation.

Solid polymer electrolytes (SPE) were obtained as follows:

LiTFSI was dissolved at room temperature in the liquid PEGDA and its different mixtures containing also PEEA^{236} or PEEA^{324} in the glove box (Ar atmosphere), the exact ratios are reported in table 1.

Solubility was checked by visual inspection. The Li^+ content was adjusted to keep the ratio EO units:Li constant and equal to 30:1, which yielded the molar LiTFSI values given in Table 1.

Darocur 1173 was used as a photoinitiator and was added at 3 % w/w (with respect to the amount of reactive oligomers) just before irradiation. For the preparation of planar membranes the reactive formulation was coated on a PP substrate by a 200 µm bar and placed in a quartz tube sealed in the glove box, the samples were then exposed to UV irradiation by an Hg lamp (intensity 30 mW/cm^2) for 5 minutes. To prepare samples for NMR experiments the formulations were filled in NMR tubes consisting of quartz and irradiated in the same way. All thesamples were solid and transparent after irradiation; they were then subject to an annealing treatment at 80 °C overnight in order to assure a complete polymerization.

Instrumental techniques and sample characterization

The insoluble fraction (*gel content*) of the cured products was evaluated as follows: the polymers were weighed, and subsequently extracted with $CHCl_3$ to dissolve any non cross-linked polymer. Extraction time was 24 h at room temperature. The cross-linked fraction was then calculated by dividing the mass of the dry sample after extraction by the mass of the original sample (relative error = ± 1 %).

The glass transition temperature (Tg) of the materials was evaluated by differential scanning calorimetry (DSC) with a METTLER DSC-30 (Greifensee, Switzerland) instrument, equipped with a low temperature probe. Samples were put in aluminium pans, prepared in a dry glove box. In a typical measurement, the electrolyte samples were cooled from ambient temperature down to -120 °C and then heated at 10 °C /min up to 120 °C. For each sample, the same heating module was applied and the final heat flow value was recorded during the second heating cycle. The Tg was defined as the midpoint of the heat capacity change observed in the DSC trace during the transition from glassy to rubbery state. The crosslinking density was evaluated by means of Dynamic-mechanical thermal analysis

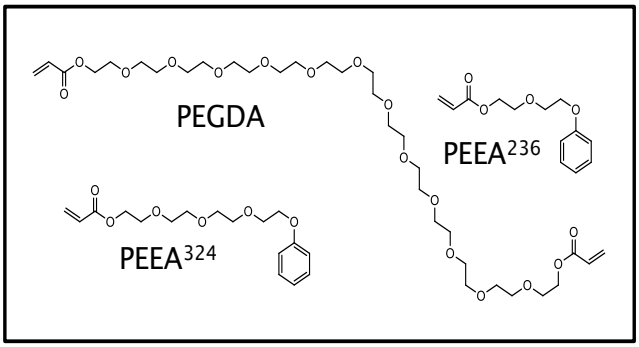

Fig.1 Structure of the chemicals PEGDA, PEEA^{324} and PEEA^{236}

Table 1 Composition in mol (%) of the samples. 3 % wt of photoinitiator was always added without being considered in the molar fractions.

	PEGDA [mol%]	PEEA^{324} [mol%]	PEEA^{236} [mol%]	LiTFSI [mol%]
PEGDA	70	---------- ---	---------- ---	30
PEGDA/PEEA^{324} (32%)	44	32	---------- ---	24
PEGDA/PEEA^{324} (56%)	26	56	---------- ---	18
PEGDA/PEEA^{236} (32%)	45	---------- ---	32	23
PEGDA/PEEA^{236} (57%)	27	---------- ---	57	16

(DMTA) with a MK III Rheometrics Scientific Instrument at 1.0 Hz frequency in the tensile configuration and heating rate of 10 °C/min. The size of the specimen was about 20×4×0.2 mm. The storage modulus, *E´*, and the loss factor, *tan δ*, were measured from -80 °C up to 80 °C.

The conductivity of the SPE membranes was determined by *electrochemical impedance spectroscopy* (EIS) analysis of cells formed by sandwiching discs of 0.785 cm^2 of the given SPE between two stainless-steel 316 (SS-316) blocking electrodes. A PARSTAT-2273 potentiostat/ galvanostat/F.R.A. (Frequency Response Analyser) instrument (Princeton Applied Research, USA) was employed for measurements at various temperatures ranging from 20 °C to 80 °C, over a 1 Hz to 100 kHz frequency range at the open circuit voltage (O.C.V.). The cells were housed in an oven (UFE-400 Memmert GmbH, Germany) to control the temperature. The resistance of the electrolyte was given by the high frequency intercept determined by analysing the impedance response using a fitting program provided with the Electrochemistry Power Suite software (version 2.58, Princeton Applied Research). Each sample was equilibrated at the experimental temperature for about 1 h before measurement. All NMR measurements were done within the temperature range 22 °C to 80 °C using a Bruker 400 MHz Avance NMR spectrometer with a liquid state probe (Bruker, Diff30) with a maximum gradient strength of 11.8 Tm^{-1} for diffusion measurements. The temperature was calibrated by a GMH 370 controller with a Pt 100 thermocouple and it is controlled with a precision of 0.25 K. Self-diffusion coefficients were measured by pulsed field gradient NMR (PFG-NMR)[6,7] for the cation (^{7}Li), the anion (^{19}F)

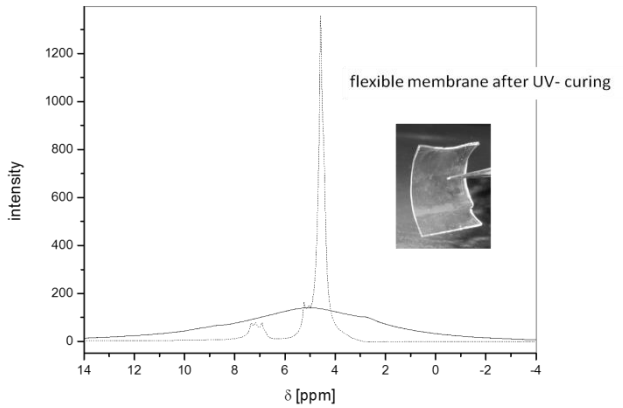

Fig.2 ^{1}H-Spectra of PEGDA before (broken line) and after (solid line) UV-irradiation.

and the polymer (^{1}H), respectively, using selective RF inserts and a stimulated echo sequence with gradient pulses.

Signal analysis was performed on the peak area of the ^{7}Li, ^{19}F or the ^{1}H signal of the oligo ether side chain, respectively. The decay of the area as a function of the gradient strength g resulted in the diffusion coefficient by fitting the exponential decay function

$$I(g) = I_0 e^{[-\gamma^2 g^2 \delta^2 D(\Delta - \frac{\delta}{3})]}, \qquad (1)$$

where δ is the gradient pulse length and Δ the observation time. Diffusion echo decays were well described by a single exponential fit, resulting in the diffusion coefficient *D*.

The spin-lattice relaxation time T_1 was measured in the same probe head using the inversion recovery sequence. The 180° pulse length was 4,5 µs for ^{1}H, 6,5 µs for ^{19}F and 11,5 µs for ^{7}Li. Signal recoveries were exponential and analyzed according to equation (2).

$$M = M_0[1 - 2e^{(\frac{-t}{T_1})}] \qquad (2)$$

Results

Characterization of the crosslinked polymers

The reactive oligomer for the preparation of the solid polymer electrolyte membranes was poly(ethylene glycol)diacrylate PEGDA, (see Figure 1), an acrylic based di-functional oligomer having an average molecular weight of 700 and containing 13 ethoxy units. Its reactivity under irradiation in the presence of a radical photoinitiator is well known. In our experimental conditions quantitative conversion of the acrylic double bonds was assured and self standing and easy to handle membranes were obtained, see inset in Fig. 2. Besides routine FTIR analyses, the successful polymerization can be visualized using 1H-spectra. In Figure 2 two spectra of the PEGDA-oligomer are shown. One is taken before UV-irradiation (broken line), the other after five minutes Similar spectra were recorded when copolymers were prepared by curing PEGDA and a monofunctional comonomer, a poly(ethylene glycol) phenyl ether acrylate (see Figure 1) i.e.

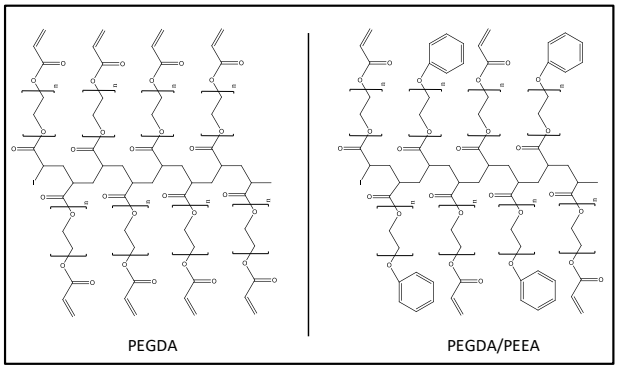

Fig.3 Crosslinking in PEGDA and PEGDA/PEEA-membranes.

of irradiation (solid line). A significant line broadening can be observed after UV-irradiation, which is due to dipolar coupling of the protons in the polymer chain. This is the typical behavior of solids PEEA^{236} or PEEA^{324} having average M_n of 236 (2 EO units) and 324 (4 EO units), respectively.

The gel content of the different networks was determined. The results are shown in Table 2. For the series of membranes a gel content in the range 87-92% is found after irradiation. Annealing the cured samples at 80°C improves the gel content: as a result of the higher mobility of the polymer at higher temperature the polymerisation process is allowed to continue and reach higher crosslinking conversion, therefore enhancing the insoluble fraction of the network .

The T_g of the networks have been obtained by DSC analysis and are reported in Table 2, measurements have been performed on the SPEs studied in this work and on the same systems without the Li salt in order to observe the influence of the latter on the mobility of the polymer chains.

As the results show, by adding the monofunctional monomers the T_g values slightly increase for both systems, with and without Li salt. Data obtained as maximum of the tan (δ) curve from DMTA confirm the same trends (not shown). T_g values are in the expected range for this kind of crosslinked systems.[30, 31] Although differences among the T_g values are within the experimental error a slight increase of T_g with the monofunctional content can be noticed. As reported for the case of poly(ethylene glycol)di(methacrylate)/ ethylene glycol phenyl ether acrylate (1EO unit) (PEGDMA/EEA) systems at various EEA content[32], the increase is explained with a reduced mobility due to the presence of stiff chain ends causing a higher T_g: the phenyl group hinders mobility and reduces the chain flexibility for monofunctional side chains. Furthermore, the length of the EO side chain of the monofunctional monomer influences the T_g-value: For a fixed monofunctional content T_g is higher when the EO side chain is shorter. This was also observed by Safranky et al. [32, 33] and by Kusuma et al [34]

In presence of LiTFSI, T_g further increases. It is known from studies of similar PEO-based solid electrolytes [10, 35] that the incorporation of a lithium salt can restrict the chain mobility as well as reduce the free volume of the final membrane, thus leading to an increase of the glass transition temperature. The trend observed between the different samples is the same with and without salt, indicating that the LiTFSI influence does not

depend on the network architecture. By DMTA analysis the

Table 2 Characteristics of the solid polymer electrolytes

Membrane	Gel content [%]		Crosslinking density ν (mmol/cm^3)	T_g (°C)	
	before annealing	after annealing		with no LiTFSI	with LiTFSI
PEGDA	92 ± 1	94 ± 1	4.2 ± 0.5	-45 ± 3	-32 ± 3
PEGDA/PEEA^{324} (32 mol%)	94 ± 1	96 ± 1	2.7 ± 0.5	-43 ± 3	-28 ± 3
PEGDA/PEEA^{324} (56 mol%)	87 ± 1	94 ± 1	2.3 ± 0.5	-41 ± 3	-26 ± 3
PEGDA/PEEA^{236} (32 mol%)	89 ± 1	97 ± 1	4.2 ± 0.5	-39 ± 3	-26 ± 3
PEGDA/PEEA^{236} (57 mol%)	88 ± 1	95 ± 1	3.2 ± 0.5	-38 ± 3	-22 ± 3

cross linking density of the networks has also been evaluated. From the statistical theory of rubber elasticity, the number of moles of crosslinked chains per unit volume, also known as the strand density, for an affine network is given by

$$E' = \nu RT \qquad (3)$$

where ν is the crosslinking density, R is the universal gas constant, and T is the absolute temperature. [36] The value of E' is chosen at a temperature T where the rubbery plateau is achieved, i.e. at a temperature much higher than T_g. In our case T was set at 40°C. The values of ν calculated by equation (3) are reported in table 2. They are quite different for the different membrane compositions. The PEGDA-membrane has the highest crosslinking density as expected. For the binary mixtures PEGDA/PEEA^{324} the density decreases strongly in dependence of the amount of PEEA^{324} and is reduced by about 50 % for the highest PEEA^{324} content.

This decrease is expected, since the PEEA-oligomers possess only one polymerizable end group and therefore the average chemical functionality of the system is reduced, which causes a lower crosslinking density. This is shown schematically in Figure 3. The addition of the shorter PEEA monofunctional units has a less pronounced influence on the crosslinking density. For low PEEA^{236} contents, the crosslinking density does not vary, at content of 57 % PEEA it is reduced by 20 %. PEEA ^{236} contains a bulky phenoxy group and only two EO units. In the presence of a shorter EO chain it is more likely to have stacking of the phenyl groups as a consequence of bond interactions. These interactions, already discussed before for explaining the increase of Tg, seem to counteract the reduction of covalent crosslinking due to the presence of a monofunctional monomer.

Long range motion - Diffusion measurements

The signal attenuation of the PFG measurements for the different nuclei always shows an exponential behaviour, indicating a single diffusion coefficient for each mobile species. The ^{19}F measurements represent the mobilities of the TFSI ion, including ions present in uncharged LiTFSI pairs while any lithium species is detected in the ^{7}Li diffusion experiment. In Figure 4 the diffusion coefficients of both nuclei are presented in an Arrhenius plot

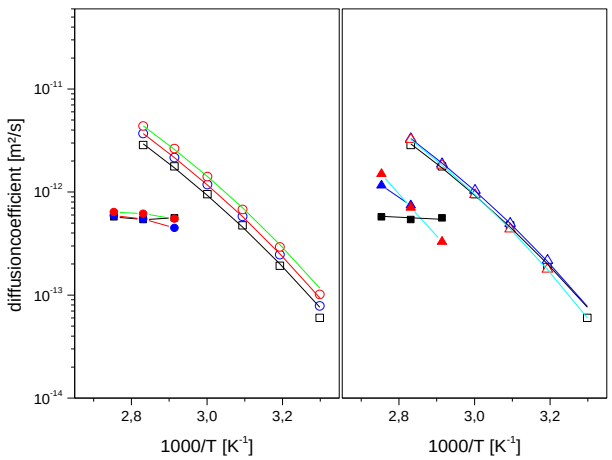

Fig.4 Diffusion coefficients of TFSI (open symbols, with VTF fits) and lithium (filled symbols; with guide to the eye lines) in dependence on temperature; neat PEGDA(black squares), 32% PEEA236 (blue triangles), 32% PEEA324(blue circles), 56% PEEA236 (red triangles), 56% PEEA324(red circles).

.

For TFSI the diffusivity increases in dependence of temperature for all membrane compositions. The studied temperature range for Li is much smaller, since the ^{7}Li signal is much weaker. Below temperatures of 60 °C - as a result of a bad signal to noise ratio and short relaxation times of ^{7}Li - only a signal attenuation by 40 % can be observed, which is not sufficient for the determination of a diffusion coefficient. In the range where *D* can be determined, it slightly increases with temperature. The diffusion of the polymer is very slow (< 10^{-14} m^2/s) and cannot be quantified, since even at high temperatures the signal attenuation is less than 10 %.

The TFSI diffusion coefficients in Fig. 4 can be described by the VTF equation:

$$D = D_0 \exp\left(\frac{-B}{T - T_0}\right) \qquad (4)$$

all samples the diffusion coefficients of lithium are much smaller than those of TFSI, though a prediction from the size of the ions would yield a much faster diffusion of the lithium. The difference

is about one order of magnitude and is a direct result of the coordination of the lithium by the oxygens of the ethylene oxide repeating units. This behaviour is typical for PEO-based electrolytes with Li salt. Several studies prove this coordination in similar PEO-based systems. The chain coordination of Li was also experimentally proven by ^{1}H-^{7}Li-COSY measurements by Judeinstein et al.[37]. In (LiTFSI)PEG$_{10}$ systems studied by Johanson et al.[19] the diffusion coefficients of the polymer and the lithium are very similar which supports the assumption of a correlated motion. In the case of an oligoether-grafted copolymer the mobilities of the chain and the lithium are very different. The chain diffusion in this poly[bis(methoxyethoxy)phosphazene] salt in polymer (MEEP) system is an order of magnitude slower compared to lithium cations[38]. In computer simulations, a coordination of the lithium by five oxygens has been determined[39].

In the systems investigated here, the influence of the monofunctional units on the ionic transport is of interest. The diffusion coefficients of ^{7}Li show interesting variations in dependence on whether PEEA^{324} or PEEA^{236} is contained. In the PEEA^{324} membranes the diffusion is less temperature dependent compared to the PEEA^{235} systems. Therefore the transport process varies with the kind of PEEA used. For both PEEA oligomers the lithium diffusion does not show variations when the amount of PEEA is increased.

In other words, in the presence of PEEA324 the diffusion coefficient of Li does not vary: the dangling chains containing 4 EO units are coordinating the cation in a similar way as the main chain does. In the presence of PEEA236 , the side chain are made of just 2 EO units. The short chains with the bulky phenyl end seem not to be able to support the coordination in the same way as the longer PEEA324 does. Indeed, in dependence on the PEEA324content the diffusion of TFSI changes: Compared to PEGDA membranes the diffusion of TFSI in PEGDA/PEEA324 membranes increases with the PEEA content. For the membranes containing the PEEA236 oligomers possible changes compared to the pure PEGDA membrane remain within error. Thus, the differences in the TFSI diffusion can be interpreted as a result of the crosslinking density shown in Table 2: A less crosslinked system, such as PEGDA/PEEA^{324} allows a higher mobility of the TFSI anion. Again, the influence of the short monofunctional unit is very small and the PEGDA/PEEA^{235} membranes show TFSI diffusion similar to that of PEGDA membranes.This is consistent with the small influence of PEEA^{236} on the crosslinking density, which was transition temperature, on the other hand, seems to have no direct influence on the anion diffusion.

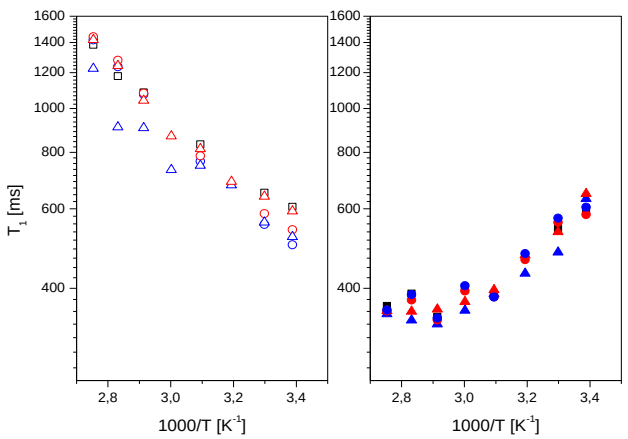

Fig.5 Relaxation times (T_1) of TFSI (open symbols) and ^{7}Li (filled symbols) in dependence on inverse temperature; neat PEGDA (black squares), 32% PEEA^{236} (blue triangles), 32% PEEA^{324}(blue circles), 56% PEEA^{236} (red triangles), 56% PEEA^{324}(red circles).

Local motions - T_1 measurements of ^{19}F and ^{7}Li

In dependence of inverse temperature, T1 relaxation times typically show a minimum. In the experimentally accessible temperature range, for ^{19}F the high temperature branch can be observed and for lithium the low temperature branch (see Figure 5). The minimum in T1 predicted by theory cannot be clearly observed for either of the nuclei, since the temperature window is limited. It is, however, evident that the minimum in T1 occurs at much higher temperature for ^{7}Li as compared to ^{19}F. Since the minimum is located at the temperature corresponding to a fixed product of the motional correlation time τ_c and the larmor frequency,[27] it can be concluded that this temperature is much lower for ^{19}F, and thus the local TFSI mobility is much higher than that of Li. This is again a common finding in PEO-based polymer electrolytes [24] and can be attributed to two reasons: One is again the Li coordination to the PEO oxygens, which reduces its local mobility. The other reason for faster local dynamics of TFSI (^{19}F) in contrast to the lithium is the free rotation around the S-C-axis. A similar effect was discussed for triflate ions in a similar polymer electrolyte environment by Kunze [38].Again, we are here interested in the influence of the mono-functional units on the local motions: For both nuclei a variation of the PEEA-content does not significantly influence the local mobility. Furthermore, a variation of the PEEA-oligomer length has no significant effect. The local environment of Li and TFSI is thus not significantly influenced by the polymer network architecture. This is consistent with the small differences observed in the Tg

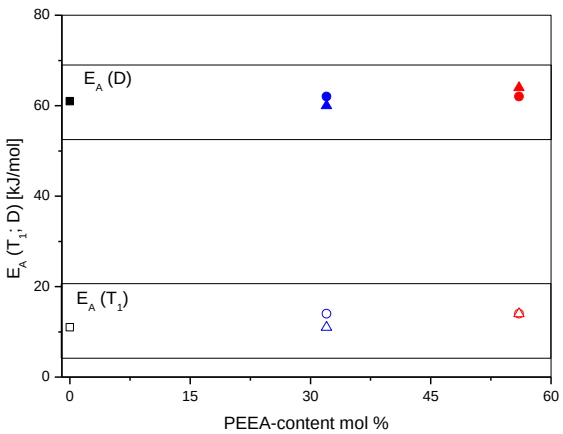

Fig.6 Activation energies of Diffusion and relaxation times TFSI (open symbols) and lithium (filled symbols) in dependence on temperature, neat PEGDA(black square), 32% PEEA^{236} (blue triangle), 32% PEEA^{324}(blue circle), 56% PEEA^{236} (red triangle), 56% PEEA^{324}(red circle) Solid lines are

representing the error range of the PEGDA data points.values of the different structures.

Activation energies

As shown in figure 5 for the T_1 relaxation of both nuclei (^{19}F, ^{7}Li), different branches can be observed. The high temperature branch observed for TFSI can be directly used to determine the activation energies of the local motions. In contrast, the slope of the low temperature branch is typically dependent on the shape of the particular spectral density function and can thus not serve

for the extraction of activation energies.[27, 40]As shown in Figure 5 for the T1 relaxation of both nuclei (19F, Figure 6 compares the activation energies of diffusion and spin-lattice relaxation for TFSI in dependence on the PEEA-content. They are obtained from fits of the raw data by the Arrhenius equation. Although the diffusion coefficients of TFSI show a slight curvature, the Arrhenius fit yields a sufficient fit quality when employing the data from 30 °C to 80 °C. It is known that the temperature dependent curvature is more pronounced to lower temperature, especially when approaching the glass transition temperature. Towards higher temperatures the curvature is flattening and can be successfully approximated by the Arrhenius law. The activation energy of diffusion is much higher compared to that of the local mobility (T1). The large difference betweendiffusion and local mobilities signifies that different processes are activated. For the diffusion it is the long range transport and for local mobilities a fast spin rotation (TFSI). The variations of EA(D) for different systems are insignificant and lie within the fitting error of ± 4 kJ/mol, indicated by the solid lines in Fig. 6. Even concerning the local mobility of TFSI, the systems do not vary significantly with the composition. Activation energies for the diffusion of the lithium ion cannot be calculated. But in view of the data presented in Figure 4 it can be assumed that in the case of the PEEA324 membranes the activation energy is much lower as compared that of the TFSI diffusion., Furthermore, it is lower in contrast to the PEEA[236] membranes in which the activation energy seems to be close to the values of TFSI.

Conductivity

The conductivities of the different membranes are shown in Figure 7. Compared to other solid electrolytes conductivities are appreciable[41]. A non-Arrhenius-like temperature dependence can be observed. Similar to the diffusion coefficients of TFSI (Figure 4), the conductivities are well described by the VFT- equation,

even though the curvature is only weak. For all compositions the conductivities increase with temperature.

. The values are typical for solid electrolytes under consideration for high temperature applications. The conductivity in PEEA[324]– containing membranes increases with PEEA content. In contrast, no effect can be observed for PEEA[236] containing membranes compared to neat PEGDA. This behaviour matches well with the result obtained from the diffusion measurements for the 19F nuclei, thus it seems that conductivity is mainly due to the TFSI anion transport. The pseudo activation energies, B, are determined using the VFT equation (5) and are summarized in Table 3.

$$\sigma = \sigma_0 \exp\left(\frac{-B}{T - T_0}\right) \tag{5}$$

For this procedure the temperature T_0 is set constant and calculated via the empirical relation

$$T_g - T_0 = 50\ \mathrm{K} \tag{6}$$

using the Tg values obtained from DSC measurements shown in Table 2.

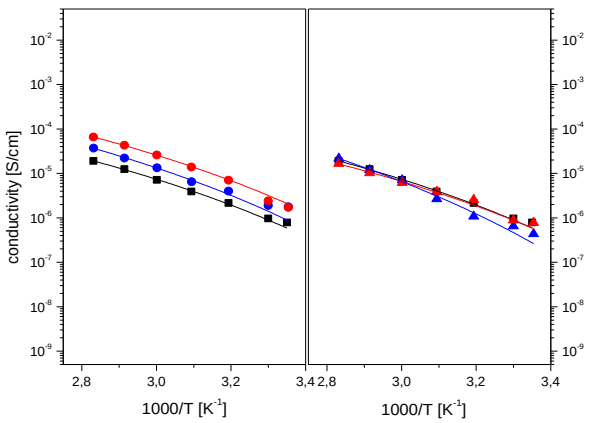

Fig.7 Ion conductivity of membranes in dependence of temperature, neat PEGDA (black square), 32% PEEA236 (blue triangle), 32% PEEA324(blue circle), 56% PEEA236 (red triangle), 56% PEEA324(red circle). Lines are VTF fits to the data employing Equ. (5).

The error for the B values is around ± 80 K. The values are very similar for the different compositions. This indicates that the energy barriers for the charge transport are similar. The same trend was observed for the values of the activation energies of the long range transport of TFSI.

Molar conductivities and degree of dissociation

The molar conductivities are calculated via the diffusion coefficients of TFSI and lithium using the Nernst-Einstein equation

$$\Lambda_{NMR} = \frac{N_A e^2}{k_B T}(D_{cation} + D_{anion}) \cdot \tag{7}$$

Table 3 Pseudo activation energies determined using the VTF-equation

	B(σdc) [K]
PEGDA	1110
PEGDA/PEEA324 (32 mol%)	1120
PEGDA/PEEA324 (56 mol%)	1010
PEGDA/PEEA236 (32 mol%)	1280
PEGDA/PEEA236 (57 mol%)	920

On the other hand, molar conductivities can be obtained from the impedance measurements by

$$\Lambda_\sigma = \frac{\sigma_{dc}}{c_{ion}} \qquad (8)$$

In this calculation, the total salt concentration is inserted as ion concentration c_{ion}, i.e. the molar conductivity calculated in this way averages over dissociated ions and non dissociated ion pairs, where the latter have a zero contribution to the conductivity. The degree of dissociation can then be expressed by the relation $R = \Lambda_{NMR}/\Lambda_\sigma$, which is plotted in Figure 8 versus the PEEA content. For all membranes the degree of dissociation is very low (<< 1 %).

Anion and cation exist in temporary average mainly as ion pairs. In literature different values for the value R can be found in PEO based electrolytes. Johanson et al. report for unbranched systems the existence of only ions, not pairs[19]. oligoether-grafted polysiloxanes a pair fraction of 90 % is estimated [38]. This value is one to two decades higher compared to the membranes reported in this paper. There are substantial differences between these three systems, for example the crosslinking density and the viscosity, which might explain the difference in *R*:

For polysiloxane salt-in-polymer electrolytes with 5 EO units (POS_5) system the crosslinking degree lies in average around 35 mmol/cm^3 [38]. Comparing with the membranes reported in this paper it can be stated that the high degree of cross-linking restricts the cation mobility and therefore supports pair formation.

The results for the PEGDA/PEEA^{324} membranes therefore show the expected trend. An increase of the number of free ions can be observed, when the crosslinking density is reduced.

In contrast, for PEEA^{236} based membranes no variation of the dissociation is found. This agrees on the one hand with the low differences in crosslinking density compared to neat PEGDA membranes and on the other hand it reflects the poor ability of short EO chains to support the coordination of lithium cations.

Discussion

We will now discuss general conclusions from all the data obtained for the PEGDA/PEEA systems. On a local scale the spin-lattice relaxation rates evidenced that the direct environment of TFSI does not depend on the membrane composition.

The TFSI activation energies are in the same range and are also very similar to the activation energies shown for PEO-PPO [26] and polysiloxane systems [38]pointing out that the anion environment is not influenced by the polymer network architecture. This is consistent with the fact that the anion is not

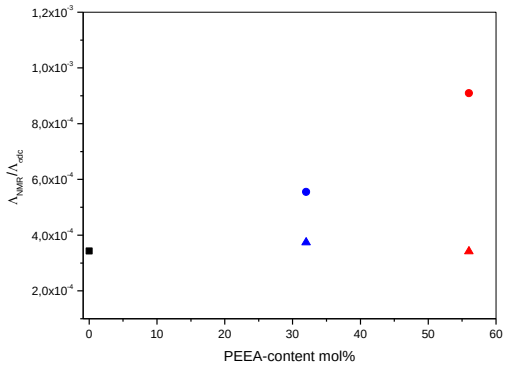

Fig.8 Value R in dependence of PEEA-content, neat PEGDA (black square), 32% PEEA236 (blue triangle), 32% PEEA324 (blue circle), 56% PEEA236 (red triangle), 56% PEEA324(red triangle).

directly coordinated to the chains, but rather interacts with the cation. The long range ion transport is influenced by the membrane architecture: Since in PEGDA and PEGDA/PEEA324 systems the lithium diffusion coefficients are very similar and almost independent on temperature, a similar diffusion mechanism with a very low activation energy can be inferred for these systems. In contrast, for PEGDA/PEEA236 membranes the temperature dependence of lithium diffusion coefficient, and thus its activation energy, is similar to that of TFSI and much higher with respect to the other systems. Thus, a different transport process seems to be relevant in these systems.

Referring to the number of available coordinating oxygens in the different PEEA oligomers it can be assumed that the longer oligomers (4 EO oxygens) will support the coordination of Lithium. In contrast, the shorter oligomers (2 EO oxygens) do not participate to the lithium coordination, but instead act as a steric hindrance for the lithium migration.

TFSI diffusion coefficients are one order of magnitude higher than those of Li and the obtained curves show a VTF behaviour indicating that the mass transport is linked to segmental motion, due to the coordination of TFSI to the cation.

Furthermore, in PEGDA/PEEA^{324} systems the TFSI diffusion increases when increasing the molar concentration of the monofunctional units. This behaviour can be related to the crosslinking density previously discussed: in a less dense network (PEGDA/PEEA^{324} systems) TFSI ions can migrate more easily from one Li to one other.

The conductivity values show the same trends as observed for TFSI diffusion, hence conductivity is mainly due to fast TFSI.

The degree of dissociation is very low for all the systems. Anion and cation are mainly existing as ion pair, and rapidly exchanging with a low fraction of salt present as single ions, which carry the current. Thus, an enhancement of the conductivity and thus improved material properties for application can be achieved by an enhancement of the degree of dissociation. The addition of a monofunctional ethyleneoxide oligomer is a successful route, as we showed here by the degree of dissociation improving with PEEA^{324} content. However, the monofunctional oligomer has to have a sufficient length, such

that it provides coordinating oxygens for the Li ion, otherwise (see PEEA[236]), no improvement is generated.

Conclusions

The crosslinked membranes presented in this paper reveal an appreciable conductivity compared to other SPEs and have the advantage of a rapid preparation. Conductivity and ion mobility are enhanced when adding a monofunctional monomer, provided that it has a sufficient length. Then, the strong reduction of crosslinking density and the coordination ability of the monofunctional provide this improvement.

The local lithium mobility is unaffected by an increase of the amount of monofunctional. However, different transport processes are revealed when varying the length of PEEA units. The mobility of lithium is strongly affected by its coordination to the PEO chains. In contrast, the mobility of TFSI is enhanced with reduced crosslinking and hence the conductivity. This might be due to a larger free volume in the PEEA[324]-membranes.

Notes and references

[a] *DISAT Politecnico di Torino, Corso Duca degli Abruzzi, 24 – 10129 Torino, Italy Fax: 0039 (0)11 0904699; Tel: 0039 (0)11 0903422; E-mail: annalisa.chiappone@iit.it*
[b] *Institut für Physikalische Chemie, University of Muenster Corrensstr. 28/30, 48149 Münster, Germany*

Aknowldgments

This work was funded in part by the VIGONI program of DAAD and CRUI, Project ID 50729094

References

1. T. Iwahori, I. Mitsuishi, S. Shiraga, N. Nakajima, H. Momose, Y. Ozaki, S. Taniguchi, H. Awata, T. Ono and K. Takeuchi, *Electrochimica Acta*, 2000, **45**, 1509-1512.
2. B. Scrosati, *Nature*, 1995, **373**, 557-558.
3. B. Scrosati, *The Chemical Record*, 2005, **5**, 286-297.
4. S. G. Chalk and J. F. Miller, *Journal of Power Sources*, 2006, **159**, 73-80.
5. J. M. Tarascon and M. Armand, *Nature*, 2001, **414**, 359-367.
6. A. S. Arico, P. Bruce, B. Scrosati, J.-M. Tarascon and W. van Schalkwijk, *Nat Mater*, 2005, **4**, 366-377.
7. J.P.Fouassier, *Photoinitiation, Photopolymerization, and Photocuring Fundamentals and Applications*, Hanser Publishers, New York, 1995.
8. M.-K. Song, J.-Y. Cho, B. W. Cho and H.-W. Rhee, *Journal of Power Sources*, 2002, **110**, 209-215.
9. C. Gerbaldi, J. Nair, C. B. Minella, G. Meligrana, G. Mulas, S. Bodoardo, R. Bongiovanni and N. Penazzi, *J Appl Electrochem*, 2008, **38**, 985-992.
10. J. R. Nair, C. Gerbaldi, M. Destro, R. Bongiovanni and N. Penazzi, *Reactive and Functional Polymers*, 2011, **71**, 409-416.
11. J. R. Nair, C. Gerbaldi, G. Meligrana, R. Bongiovanni, S. Bodoardo, N. Penazzi, P.Reale and V. Gentili, *Journal of Power Sources*, 2008, **178**, 751-757.
12. C. Gerbaldi, *Ionics*, 2010, **16**, 777-786.
13. J. P. Baltaze and P. Judeinstein, *Solid State Ionics*, 2010, **181**, 672-677.
14. A. L. B. S. Bathista, E. R. deAzevedo, A. C. Bloise, K. Dahmouche, P. Judeinstein and T. J. Bonagamba, *Chemistry of Materials*, 2007, **19**, 1780-1789.
15. L. van Wüllen, T. K. J. Köster, H.-D. Wiemhöfer and N. Kaskhedikar, *Chemistry of Materials*, 2008, **20**, 7399-7407.
16. P. Judeinstein and C. Sanchez, *Journal of Materials Chemistry*, 1996, **6**, 511-525.
17. S. Arumugam S , J Tunstall D Pand Vincent C A, *Journal of Physics: Condensed Matter*, 1993, **5**, 153.
18. J. P. Donoso, T. J. Bonagamba, H. C. Panepucci, L. N. Oliveira, W. Gorecki, C. Berthier and M. Armand, *The Journal of Chemical Physics*, 1993, **98**, 10026-10036.
19. A. Johansson, A. Gogoll and J. Tegenfeldt, *Polymer*, 1996, **37**, 1387-1393.
20. T. Eschen, J. Kösters, M. Schönhoff and N. A. Stolwijk, *The Journal of Physical Chemistry B*, 2012, **116**, 8290-8298.
21. J. Fögeling, M. Kunze, M. Schönhoff and N. A. Stolwijk, *Physical Chemistry Chemical Physics*, 2010, **12**, 7148-7161.
22. I. M. Ward, N. Boden, J. Cruickshank and S. A. Leng, *Electrochimica Acta*, 1995, **40**, 2071-2076.
23. D. J. Roach, S. Dou, R. H. Colby and K. T. Mueller, *The Journal of Chemical Physics*, 2012, **136**, 014510.
24. M. Kunze, Y. Karatas, H.-D. Wiemhöfer, H. Eckert and M. Schönhoff, *Physical Chemistry Chemical Physics*, 2010, **12**, 6844-6851.
25. K. Hayamizu, Y. Aihara and W. S. Price, *The Journal of Chemical Physics*, 2000, **113**, 4785-4793.
26. K. Hayamizu, Y. Aihara and W. S. Price, *Electrochimica Acta*, 2001, **46**, 1475-1485.
27. P. A. Beckmann, *Physics Reports*, 1988, **171**, 85-128.
28. O. Söderman, W. S. Price, M. Schönhoff and D. Topgaard, *Journal of Molecular Liquids*, 2010, **156**, 38-44.
29. W. S. Price, *Concepts in Magnetic Resonance*, 1997, **9**, 299-336.
30. J. A. Killion, L. M. Geever, D. M. Devine, J. E. Kennedy and C. L. Higginbotham, *Journal of the Mechanical Behavior of Biomedical Materials*, 2011, **4**, 1219-1227.
31. S. Kalakkunnath, D. S. Kalika, H. Lin, R. D. Raharjo and B. D. Freeman, *Polymer*, 2007, **48**, 579-589.
32. D. L. Safranski and K. Gall, *Polymer*, 2008, **49**, 4446-4455.
33. G. Pizzirani, P. Magagnini and P. Giusti, *Journal of Polymer Science Part A-2: Polymer Physics*, 1971, **9**, 1133-1145.
34. V. A. Kusuma, S. Matteucci, B. D. Freeman, M. K. Danquah and D. S. Kalika, *Journal of Membrane Science*, 2009, **341**, 84-95.
35. W. Wieczorek, J. R. Stevens and Z. Florjańczyk, *Solid State Ionics*, 1996, **85**, 67-72.
36. J.-S. Chen, C. K. Ober, M. D. Poliks, Y. Zhang, U. Wiesner and C. Cohen, *Polymer*, 2004, **45**, 1939-1950.
37. P. Judeinstein, D. Reichert, E. R. DeAzevedo and T. J. Bonagamba, *Acta Chimica Slovenica*, 2005, **52**, 349-360.
38. M. Kunze, A. Schulz, H.-D. Wiemhöfer, H. Eckert and M. Schönhoff, *Zeitschrift für Physikalische Chemie*, 2010, **224**, 1771-1793.
39. A. Maitra and A. Heuer, *The Journal of Physical Chemistry B*, 2008, **112**, 9641-9651.

40. M. Grüne, W. Müller-Warmuth, P. zum Hebel and B. Krebs, *Solid State Ionics*, 1993, **66**, 165-173.
41. J. W. Fergus, *Journal of Power Sources*, 2010, **195**, 939-954.